American Geophysical Union (AGU) fall meeting. December 1st-7th, 2020

Solar Induced Chlorophyll Fluorescence and Vegetation Indices for Heat Stress Assessment in Three Crops at Different Geophysics-Derived Soil Units

J. Quiros[1], C. Brogi[2], V. Krieger[1], B. Siegmann[1], M. Celesti[3], M. Rossini[3], S. Cogliati[3], L. Weihermueller[2] and U. Rascher[1]

Forschungszentrum Jülich, Institutes for Bio- and Geosciences IBG-2 (Plant Sciences[1]) and IBG-3 (Agrosphere[2]); and the Department of Earth and Environmental Sciences, University of Milano – Bicocca[3]

The solar Induced chlorophyll fluorescence (SIF) can reveal plant physiological alterations caused by biotic and abiotic stress factors, as it is directly related to photosynthesis. Alongside climatic variations, the edaphic properties of agricultural fields strongly impact the crop performance. Therefore, a match is expected between soil units and SIF spatial distribution. However, to better understand the link between those two information layers, more studies are required investigating that relation at different locations, times and crops. Thus, the objective of the present study is to employ SIF for the assessment of heat stress in three crops (potato, sugar beet and corn) growing at different geophysics-derived soil units in two edaphic region (lower and upper terraces). We also aim at: i) the comparison between SIF and three reflectance-based vegetation indices (VIs), as well as ii) its match with geophysics-derived soil spatial patterns. To achieve this, airborne hyperspectral data were recorded with the HyPlant sensor on June 29 (10:36 hrs), and August 2 (12:38 hrs) 2018 in Selhausen, West Germany. Spectral Fitting Method (SFM)-based SIF and SIFyield (SIF/APAR), as well as three VIs were computed to evaluate the impact of an heat wave during the summer-2018 on the three crops as a function of the soil units. To do this, a high resolution soil map was created, based on soil geophysics information collected with the Electromagnetic Magnetic Induction (EMI).

The study site and heat wave

The study site covers an area of around 500 ha (Figure 1). The geophysics-based soil map covers an area of 100 ha including the lower (LT) and upper (UT) terraces characteristic of the local landscape. LT and UT have distinct soil and subsoil characteristics (see later description) and are separated by a locally abrupt slope of ~10m. Three representative fields of corn, potato and sugar beet were selected in each terrace to compare the use of SIF and VIs for the assessment. Additionally, five fields (Figure 1, in blue) were selected for the comparison of SIF and soil spatial variability.

The airborne hyperspectral data were recorded on June 29 (10:36 hrs -CEST-), and August 2 (12:38 hrs -CEST-) at 600 m flight altitude. The dates correspond to the end and beginning of the peak of a heat wave occurred in 2018 (Figure 2a). Both datasets were collected under comparable PAR conditions (Figure 2b). The geophysical information was obtained with a six receivers CMD MiniExplorer electromagnetic induction (EMI) instrument (GF instruments, Brno, Czeck Republic). Geophysical data were later combined with direct soil sampling information. Brogi et al. 2018 (DOI: 10.1016/j.geoderma.2018.08.001) and Brogi et al. 2020 (DOI: 10.1002/vzj2.20009) describe in detail this 2016-data collection as well as the mapping process.

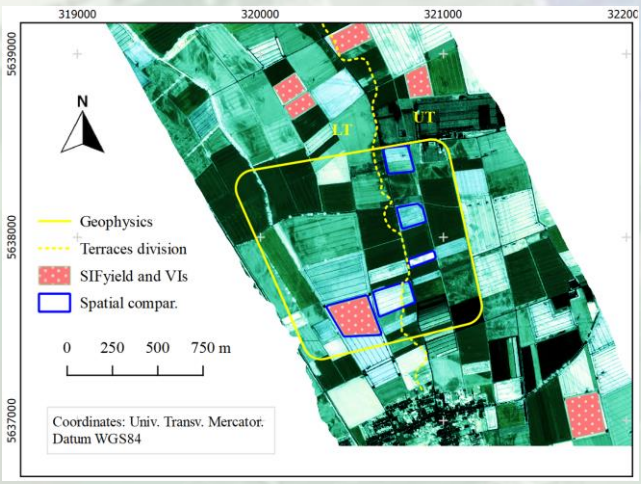

Figure 1: Location of the area covered by the geophysics map (yellow line) and the terraces division line (dotted yellow line, LT=lower terrace, UT=upper terrace), as well as the fields used for SIFyield and VIs computation (filled red polygons) and the spatial relation analysis (blue polygons) over an example airborne overpass.

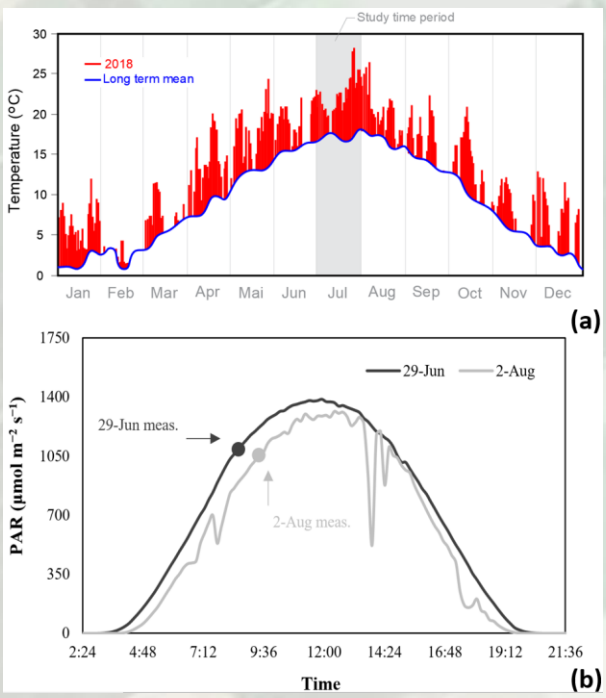

Figure 2: (a) 2018 temperature from a local meteo station (red bars) above the long-term mean temperature curve (in blue). (b) photosynthetic active radiation (PAR) in 10 minute intervals for the two days with corresponding HyPlant overpasses.

Computation of SIF & VIs from the HyPlant sensor

The HyPlant raw imagery from the FLUO module was processed following the steps detailed in Siegmann et al. (2019; DOI: 10.3390/rs11232760). The SIF was retrieved with the latest version of the Spectral Fitting Method (SFM; Cogliati et al., 2019; DOI: 10.3390/rs11161840), which includes a bare soil pixel-based approach (Cogliati et al., unpublished). An empirical method, based on the wide dynamic range vegetation index (WDRVI, Eq. 1), was employed to calculate the Fraction of Absorbed PAR (fAPAR, Eq. 2), as per their existing linear correlation reported in Liu et al. (2019; DOI: 10.1016/j.rse.2018.05.035). The SIFyield (in the O2A and O2B absorption bands) was computed dividing SIF by into the fraction of the absorbed PAR (APAR) (Eq. 3); the latest is nothing but the product of PAR and *f*APAR.

$$\mathrm{WDRVI} = \frac{(\alpha * R_{<795-810>}) - R_{<665-680>}}{(\alpha * R_{<795-810>}) + R_{<665-680>}} \quad \textbf{Eq. 1}$$

$$fAPAR = (0.516 * \mathrm{WDRVI}) + 0.726 \quad \textbf{Eq. 2}$$

$$SIF_{yield} = \frac{\mathrm{SIF}}{f\mathrm{APAR} * \mathrm{PAR}} \quad \textbf{Eq. 3}$$

Where α is a weighing coefficient from 0.10-0.20. For the present study an α value of 0.15 was selected. The R represents the reflectance at the specified subscripted wavelength. The MERIS terrestrial chlorophyll index (MTCI; Dash et al. 2004; DOI: 10.1080/0143116042000274015) and the photochemical reflectance index (PRI; Gamon et al., 1992; DOI: 10.1016/0034-4257(92)90059-S) indices were calculated with Eq. 4 and 5, respectively.

$$\mathrm{MTCI} = \frac{R_{<754\pm7.5>} - R_{<709\pm10>}}{R_{<709\pm10>} - R_{<681\pm10>}} \quad \textbf{Eq. 4}$$

$$\mathrm{PRI} = \frac{R_{<570\pm2.5>} - R_{<531\pm2.5>}}{R_{<570\pm2.5>} + R_{<531\pm2.5>}} \quad \textbf{Eq. 5}$$

How did SIF & VIs assess the impact of the heat?

Maps of SIFyield (Eq. 3) at the O2-A and O2-B bands for June 27 and August 2 are shown in Figure 3. The average (± standard deviation -SD-) SIFyield A and B, MTCI, PRI and normalized difference vegetation index (NDVI) of potato, sugar beet and corn fields on June 27 and August 2 are presented in Figure 4. The results are also differentiated according to the field location, whether they are in the lower or upper terrace. The time of the flight-line acquisition is also highlighted by the used border bar line types.

At the beginning of the heat wave we found that, compared with VIs, SIF data showed a clearer differentiation of the stress conditions at the terrace level for potato and sugar beet. Moreover, towards the end of the heat wave a significant decrease of MTCI and NDVI contrasted with higher SIF in sugar beet and corn. Nonetheless, those crops (sugar beet and corn) did not show significant SIF differences between terraces.

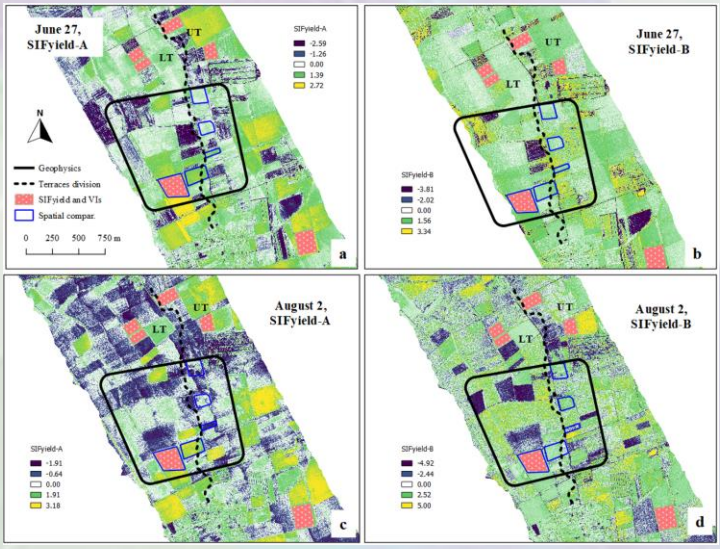

Figure 3: SIFyield-A and B output mosaics of June 27 (a and b) and August 2 (c and d) with the geophysics map (black line) and terraces boundaries (dotted black line), as well as the fields used for SIFyield (solid red polygons) and spatial similarity (blue polygons) analysis overlaid.

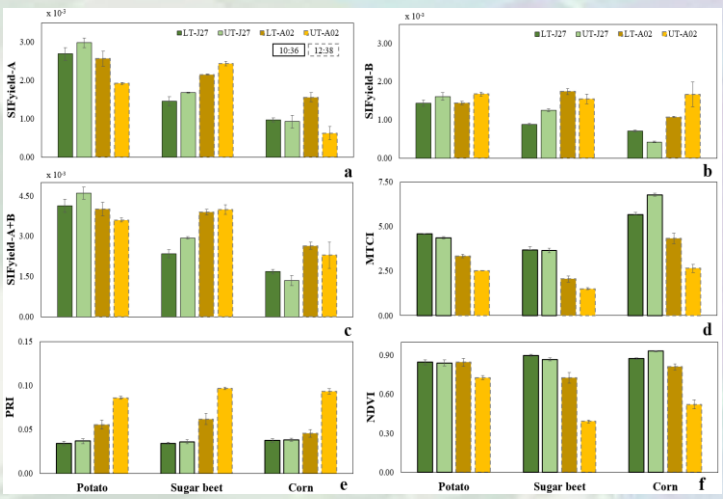

Figure 4: SIFyield-A (a), SIFyield-B (b), SIFyield-A+B (c), MTCI (d), PRI (e) and NDVI (f) of the three crops (potato, sugar beet and corn) in the lower (LT) and upper (UT) terraces before (BH) and after the peak of the heat stress (AH). The time of both HyPlant overpasses are also highlighted in black (BH) and dotted (AH) bar border lines.

How did the SIF & Soil maps spatially relate?

The soil of the mapped area was divided into 15 units regarding horizon distribution across the vertical profile (Figure 5). The detailed description of each soil unit and horizon edaphic properties can be found in Brogi et al. (2018). The Figure 5b presents the soil unit maps for the five fields selected to compare with the spatial variability of SIFyield. Panels b and c of Figure 5 show the respective SIF-B and NDVI maps of those fields, with the respective date clarified. Fields 1, 2 and 4 present similar soil and SIF-B spatial patterns that are also visible in the NDVI data. Interestingly, on Fields 3 and 5 the SIF map patterns matched with the soil units shape more clearly than the NDVI. The latter may indicate that the greenness/vigor data given by indices like the NDVI does not provide the same information about the real physiological stress status of plants as SIF. Particularly, in the Field 5 on August 2, e.g., the higher SIF in the UT is associated to the higher impact of heat stress evidenced with the PRI data; in a moment when the NDVI map was homogeneous.

In addition, Figure 6 shows a map of the SIF-B and NDVI of the fields 3 (a and b) and 5 (e and f), and the statistical difference (p value) between soil classes (tables, c and g). SIF maps for June 26, 2019, are presented in Figure 6d and h. In order to offer an idea of the consistency of SIF vs. geophysics-based soil units spatial match, Figure 6 (d and h) includes 2019 maps of the two main fields (3 and 5).

The differences among soil classes, in the present study, are mostly related to the depth of ancient river beds represented as the sand&gravel horizon which has poorer hydraulic properties compared to the topsoil (Borgi et al., 2020). In general, the shallower this sand&gravel horizon (e.g. in A1d and D1d units) the lower is the water availability, thus the strongest the impact of heat stress. In counterpart, crops tend to grow healthier at soil units like the A1a and D1a, where the sand&gravel horizon is deeper. Spatial patterns related to stress would not be expected in soil units classified within groups B and C, without the presence of the river bed horizon. Nonetheless, the exceptional dry conditions of 2018 influenced to see some patterns, e.g. in the Field 4, that are probably caused by more subtle differences in soil properties

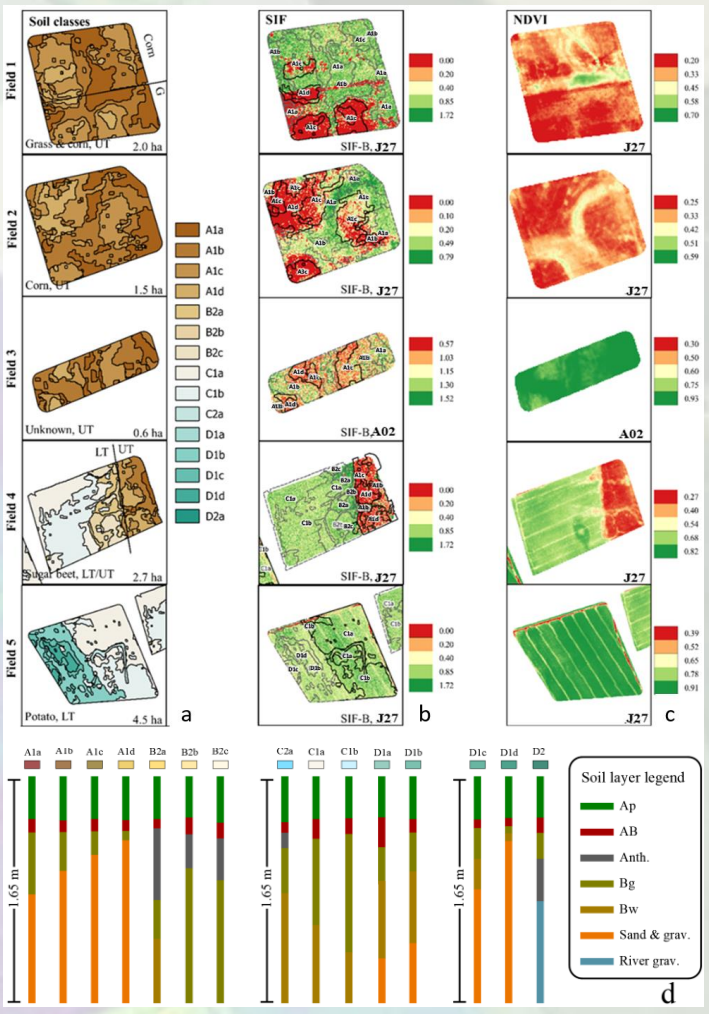

Figure 5: Geophysics-derived soil classes (a), SIF (b), and NDVI (c) maps of the five fields used for the comparison of SIF and soil spatial patterns. The soil profiles derived at 1.65 m depth per geophysics-derived class are presented in (d).

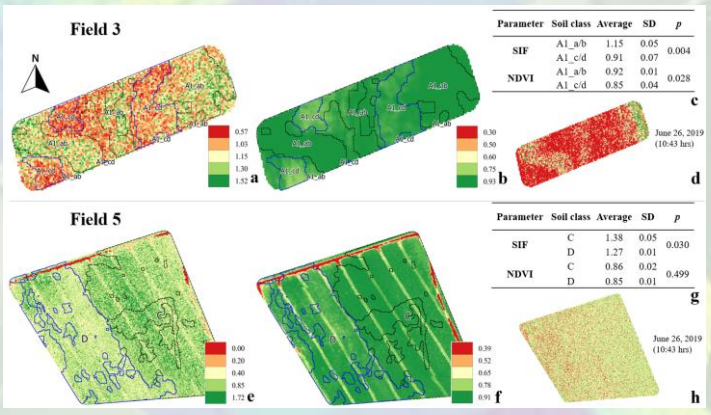

Figure 6: SIF-B and NDVI maps of fields 3 (a and b) and 5 (e and f), and their respective difference between soil classes using means-comparison (tables, c and g). June 26, 2019, SIF maps are presented (d and h).

Outcome statements

- At the beginning of the heat wave we found that, compared with VIs, SIF data showed a clearer differentiation of the stress conditions at a terrace level in potato and sugar beet.
- Towards the end of the wave a significant decrease of MTCI and NDVI contrasted with higher SIF in sugar beet and corn. Nonetheless, those crops (beet and corn) did not show significant SIF differences between terraces.
- A significant spatial match was found between SIF and geophysics-derived soil spatial patterns (p = 0.004-0.030) in fields where NDVI was more homogeneous (p = 0.028-0.499, respectively). This suggests the higher sensitivity of SIF to monitor heat stress compared with common VIs.

Further ongoing research

Further ongoing research: in order to better understand the spatial relation between the SIF and soil maps, (i) quantitative information about soil water available for plants, and (ii) satellite-based evapotranspiration data will be incorporated into the analysis. Moreover, the new analysis will include multiple year SIF data aiming at more robust results.

***Funding**: The research has received funding from the European Union's Horizon 2020 research and innovation program under the Marie Sklodowska-Curie grant agreement no. 721995. This document was prepared within the Training on Remote Sensing for Ecosystem Modelling (TRuStEE) consortium.*

The presented research aims to be as well a parallel contribution within the frame of the European Space Agency (ESA) project: "PhotoProxy".